OpenAIR@RGU

The Open Access Institutional Repository
at Robert Gordon University

http://openair.rgu.ac.uk

This is an author produced version of a paper published in

Proceedings of the Institution of Mechanical Engineers, Part A: Journal of Power and Energy (ISSN 0957-6509, eISSN 2041-2967)

This version may not include final proof corrections and does not include published layout or pagination.

Citation Details

Citation for the version of the work held in 'OpenAIR@RGU':

Citation for the publisher's version:

Laminar Flamelet Model Prediction of NO$_x$ Formation in a Turbulent Bluff-body Combustor

M. Ravikanti

Wolfson School of Mechanical and Manufacturing Engineering,
Loughborough University, Loughborough, LE11 3TU, UK

Phone: 01509 227520, Fax: 01509 227648
Email: S.M.Ravikanti-Veera-Venkata@lboro.ac.uk

M. Hossain*

School of Engineering, The Robert Gordon University,
Schoolhill, Aberdeen, AB15 9QE

Phone: 01224 262351 Fax: 01224 262444
Email: M.Hossain@rgu.ac.uk

W. Malalasekera

Wolfson School of Mechanical and Manufacturing Engineering
Loughborough University, Leicestershire, LE11 3TU, UK

Phone: 01509 227556, Fax: 01509 227648
Email: W.Malalasekera@lboro.ac.uk

* Corresponding Author

Abstract

Bluff body combustor, with recirculation zone and simple boundary conditions, is ideal as a compromise for an industrial combustor for validating combustion models. This combustor, however, has proved to be very challenging to the combustion modellers in a number of previous studies. In the present study, an improved prediction has been reported through better representation of turbulence effect by Reynolds stress transport model and extended upstream computational domain. Thermo-chemical properties of the flame have been represented by a laminar flamelet model. Comparison among reduced chemical kinetic mechanism of Peters and detailed mechanisms of GRI 2.11, GRI 3.0 and San Diego has been studied under the laminar flamelet modelling framework. Computed results have been compared against the well-known experimental data of Sydney University bluff-body CH_4/H_2 flame. Results show that the laminar flamelet model yields very good agreement with measurements for temperature and major species with all the reaction mechanisms. The GRI 2.11 performs better than the other reaction mechanisms in predicting minor species such as OH and pollutant NO. The agreement achieved for NO is particularly encouraging considering the simplified modelling formulation utilised for the kinetically controlled NO formation.

Keyword(s): Bluff-body; combustion; laminar flamelet; NOx prediction

Introduction

Fundamental understanding of combustion process is of paramount importance not only for achieving better thermal efficiency but also for reducing pollutant emissions. Nitrogen oxides (NO_x), emitted during combustion reactions, are environmental hazard as they create problems such as acid rain and depletion of ozone in stratosphere. To develop low NO_x combustor, a better understanding of formation of NO_x in turbulent flames is essential. Although route to NO_x formation and associated chemical kinetics are well known, the interaction between the chemical reactions and turbulence is less understood. An advanced combustion model is needed that takes into account complex processes involving detailed chemistry and non-equilibrium effect in order to be successful in predicting NO_x emission.

Turbulence-chemistry interaction has been a major focus of the combustion researchers for the last decades. Scalar variables such as temperature and concentrations of species are a unique function of a conserved scalar variable, mixture fraction, in a turbulent reacting flame [1]. Once the mixture fraction and its fluctuations are known in a turbulent flame, the averaged scalar variable can be obtained by integration of scalar variable functions with a presumed probability density distribution of mixture fraction. This simplified fast chemistry-based approach is however inadequate to predict minor species such as OH and O. Accurate prediction of OH and O is the first step in successful prediction of NO_x. An advanced modelling approach is therefore required to predict NO_x emissions from a turbulent flame. Laminar flamelet model is one such advanced model. Laminar flamelet model is based on the premise that a turbulent flame can be represented by an ensemble of "laminar flamelets", which are stretched by turbulence [2,3]. In this modelling framework, a library of laminar flamelets is generated by solving transport equations on one-dimensional laminar flame configuration. Alternatively, a laminar flamelet equation on a mixture fraction space can be derived by Crocco transformation [4]. Since the flamelet equations are solved for

laminar flow, detailed chemical reaction mechanism can be used for generating flamelet library. The generated flamelet library is then linked to the reacting turbulent flow field through a variable known as scalar dissipation rate. The effect of turbulence is thus decoupled from the chemistry with significant reduction of computational complexity. Conditional Moment Closure (CMC) [5] and transported PDF [6,7] models are other advanced models that have gained attention of many researchers. The CMC model is based on solution of conditional average equations of random reacting variables. Success of the CMC model depends largely on the adequate modelling of conditional moment of scalar variables in the Arrhenius reaction term. The transported PDF model does not require a model to represent the Arrhenius reaction term, but it requires a model to represent the mixing rate. The accuracy of the model depends on adequate modelling of the mixing rate. Though the model is theoretically more advanced, the model still has shortcomings in predicting many features of turbulent flames such as local extinction [8].

Accurate prediction of formation of oxides of nitrogen especially NO in turbulent nonpremixed flames has been a challenge to combustion modellers. There have been a number of recent studies in the formation of NO in both jet and bluff-body flames. Barlow et al [9] reported a H_2/He jet flame prediction of NO using a transported PDF model. In their study, the transported PDF model produced better prediction of NO than a first order CMC prediction. The same flame was also investigated by Kronenburg et al [10] using a second order CMC model. They reported good prediction for NO. Roomina and Bilger [11] reported a first order CMC study of a CH_4/air jet flame with reasonable accuracy for NO prediction. Mahmud et al [12] reported an experimental and computational study of a CH_4 jet flame. Their calculation using a mixedness-reactedness flamelet model showed large overprediction of NO in the fuel rich zone. Hossain and Malalasekera [13] reported the prediction of NO in a bluff-body CH_4/H_2 flame using a steady laminar flamelet model. Their prediction suffered from accounting only thermal route and showed large underprediction of NO level. Kim and Huh [14] reported a first order CMC modelling study of the same bluff-body flame

using Miller-Bowman, GRI 2.11 and 3.0 mechanisms. Their simulation showed that the GRI 2.11 and Miller-Bowman mechanism yielded reasonable agreement with NO measurement. However, the GRI 3.0 produced large overprediction. Sreedhara and Huh [15] compared 1st and 2nd order CMC model for the same bluff-body flame. They reported that the 2nd order CMC model improved the NO prediction, but still showed considerable overprediction.

The same bluff-body flame has been studied numerically by a number of researchers focusing on turbulence model. Dally et al [16] reported simulation results obtained using the standard and a modified $k - \varepsilon$ and Reynolds stress models. The main focus of their work was on the prediction of flow field, and both the $k - \varepsilon$ and Reynolds stress models in the standard form failed to predict the flow field sufficiently accurately. The value of turbulence model constant of $C_{\varepsilon 1} = 1.6$ was proposed to improve the prediction of flow field. Merci et al [17] applied a new cubic nonlinear eddy viscosity turbulence model to predict this flame. Their prediction showed that improvements in the flow field prediction using the new cubic model was only modest. Li et al [18] investigated this flame using various differential Reynolds stress models. They reported that all the differential stress models in the standard form failed to reproduce the mean velocity, velocity fluctuations, mean mixture fraction and its variances. Modification to turbulence model constant led to minor improvements of the mean mixture fraction and variance profiles in upstream locations. However, the mean mixture fraction profiles were severely underpredicted at downstream locations. Yan et al [19] provided a turbulence model sensitivity study using the standard $k - \varepsilon$ model, the explicit algebraic stress model and the $k - \varepsilon$ model with varied anisotropy parameters. Their study provided a very good prediction of mixture fraction profiles at upstearm locations, though there was slight overprediction near the centreline. The mixture fraction profiles were underpredicted at downstream locations. The prediction of mixture fraction variances as well as velocity fluctuations was not good. This bluff-body flame has also been studied using LES turbulence models [20, 21].

The LES model calculation failed to predict the flow field in the farfield in Kempf et al's study [20]. However, Raman and Pitsch [21] provided a much better prediction using a recursive filter-refinement procedure (RFRP) for LES. It is noteworthy that almost all of the approaches mentioned above needed modifications to the standard value of the model constants to provide a good prediction.

This paper reports a numerical modelling study of the detailed structure of a CH_4/H_2 bluff-body flame. The predictions from laminar flamelet model with Peters, GRI 2.11, GRI 3.0 and San Diego chemical mechanisms have been compared with the well-known Sydney bluff-body HM1 flame data [22]. The turbulent feature of the flame has been captured through a Reynolds stress transport model. Previous studies [16-21] have shown that the $k - \varepsilon$ model is not accurate enough to capture all the turbulence features in this flame, while the LES model is more demanding on computing resources without providing much improvement in the prediction. The Reynolds stress model, therefore, provides a good compromise between the accuracy and computing resources.

Mathematical Model

Thermofluids

Reynolds averaged Navier-Stokes equations in conjunction with equations pertaining to the turbulence and combustion models have been solved using an in-house finite volume code. A brief description of the relevant governing equations and the modelling concept is presented here.

Overall mass continuity equation:

$$\frac{\partial \overline{\rho}\widetilde{u}_j}{\partial x_j} = 0 \qquad (1)$$

Momentum conservation equation:

$$\frac{\partial}{\partial x_j}\left(\bar{\rho}\tilde{u}_j\tilde{u}_i\right) = -\frac{\partial\bar{P}}{\partial x_i} - \frac{\partial}{\partial x_j}\left(\rho\overline{u_i''u_j''}\right) \qquad (2)$$

The term $\rho\overline{u_i''u_j''}$ represents turbulent or Reynolds stresses. In the present study this term has obtained from a Reynolds stress transport model.

Reynolds stress turbulence closure

The Reynolds stress transport (RST) model adopted in the present study is essentially the model proposed by Launder et al [23], but with minor modifications. The RST model involves solving modelled partial differential equations for normal stresses and shear stress. The equations governing the transport of Reynolds stresses are given in Cartesian tensor notation as:

$$\frac{\partial}{\partial x_k}\left(\tilde{u}_k\rho\overline{u_i''u_j''}\right) = D_{ij}{}^\nu + D_{ij}{}^T + D_{ij}{}^P + P_{ij} + \Phi_{ij} - \bar{\rho}\tilde{\varepsilon}_{ij} \qquad (3)$$

The term on the left hand side represents convective transport of the Reynolds stresses while the first three terms on the right hand side represent molecular, turbulent and pressure diffusion followed by production by shear, pressure-strain term and finally, stress dissipation. For high Reynolds number flows that are of interest in the present study, molecular diffusion is negligible and hence neglected. The pressure transport is considered to be much smaller than velocity transport and hence pressure diffusion has been neglected as well. In the context of the present problem, the body force and production by rotation are not pertinent and hence not considered in the transport equation.

Turbulent diffusion has been modelled using the simple gradient diffusion hypothesis (Lien and Leschziner [24]):

$$D_{ij}^{T} = -\frac{\partial}{\partial x_k}\left(\mu_T \frac{\partial \overline{u_i'' u_j''}}{\partial x_k}\right) \tag{4}$$

Production by shear has been subjected to exact treatment and is given by:

$$P_{ij} = -\left(\rho \overline{u_j'' u_k''} \frac{\partial \tilde{u}_i}{\partial x_k} + \rho \overline{u_i'' u_k''} \frac{\partial \tilde{u}_j}{\partial x_k}\right) \tag{5}$$

Pressure strain rate term is a combination of conventional Rotta's 'slow' or 'return-to-isotropy' term Φ_{ij1} and a 'rapid' pressure strain term Φ_{ij2} modelled according to Isotropization of production proposal of Naot et al [25]:

$$\Phi_{ij} = \Phi_{ij1} + \Phi_{ij2} = -C_1 \overline{\rho} \frac{\tilde{\varepsilon}}{\tilde{k}}\left(\overline{u_i'' u_j''} - \frac{2}{3}\delta_{ij}\tilde{k}\right) - C_2 \overline{\rho}\left(P_{ij} - \frac{1}{3}\delta_{ij}P_{kk}\right) \tag{6}$$

The model constants C_1 and C_2 are given the values of 1.8 and 0.6 respectively.

The dissipation rate term has been modelled using the local isotropy hypothesis of Kolmogorov which is pertinent to high Reynolds number flows.

$$\tilde{\varepsilon}_{ij} = \frac{2}{3}\overline{\rho}\tilde{\varepsilon}\delta_{ij} \tag{7}$$

The turbulent dissipation rate $\tilde{\varepsilon}$ is obtained by solving its transport equation:

$$\frac{\partial}{\partial x_k}\left(\overline{\rho}\tilde{u}_i\tilde{\varepsilon}\right) = \frac{\partial}{\partial x_k}\left(\frac{\mu_T}{\sigma_\varepsilon}\frac{\partial \tilde{\varepsilon}}{\partial x_k}\right) + C_{\varepsilon 1}\frac{\tilde{\varepsilon}}{\tilde{k}}P_{kk} - C_{\varepsilon 2}\overline{\rho}\frac{\tilde{\varepsilon}^2}{\tilde{k}} \tag{8}$$

where the rate of production of turbulent kinetic energy $P_k = 0.5P_{kk}$. The model constants take the following values: $C_{\varepsilon1} = 1.6$, $C_{\varepsilon2} = 1.44$ and $\sigma_\varepsilon = 1.3$. The standard value for the model constant $C_{\varepsilon1}$, 1.4, has been changed following the recommendation of Dally et al [16]. The turbulent kinetic energy can be obtained from the summation of normal stresses. However, to facilitate stability while solving for the Reynolds stresses, the turbulent kinetic energy has been obtained from the solution of its transport equation:

$$\frac{\partial}{\partial x_k}\left(\bar{\rho}\tilde{u}_i\tilde{k}\right) = \frac{\partial}{\partial x_k}\left(\frac{\mu_T}{\sigma_k}\frac{\partial\tilde{k}}{\partial x_k}\right) + P_k - \bar{\rho}\tilde{\varepsilon} \qquad (9)$$

where the Prandtl number for turbulent kinetic energy σ_k takes a value of 0.82 as suggested by Lien and Leschziner [24].

In Eqs.8 and 9, the turbulent fluxes have been modelled using a simple gradient diffusion hypothesis. This practice has also been adopted for scalars pertinent to combustion modelling, example, the mean mixture fraction and mean NO mass fraction. Although, the turbulent scalar fluxes could be solved by a procedure similar to that adopted for Reynolds stresses which would then lead to a full second moment closure, such an effort would involve significantly high computational times and hence the simple gradient diffusion hypothesis has been preferred.

Laminar flamelet model of combustion

In the present study, the interaction between turbulence and combustion has been handled by employing laminar flamelet model. Laminar flamelet modelling is a two-step process. In the first step, a flamelet library is created by solving flamelet equations, which are derived from conservation equations of mass, momentum, species and energy through Crocco transformation [4]. In the second step, the mean scalar variables in a turbulent flame are computed in a CFD code using the generated flamelet library.

The flamelet profiles specify temperature, density and species concentrations by the mixture fraction Z and the scalar dissipation rate at stoichiometric mixture fraction χ_{st}. For turbulent flames, the mean scalar variables are computed from the laminar flamelet relation of the mixture fraction and the scalar dissipation rate by integrating with a joint probability density function as:

$$\tilde{\phi} = \int_0^1 \int_0^\infty \phi\left(Z;\chi_{st}\right)\tilde{P}\left(Z,\chi_{st}\right)d\chi_{st}dZ \qquad (10)$$

The assumption of statistical independence between mixture fraction and scalar dissipation rate leads to $\tilde{P}\left(Z,\chi_{st}\right) = \tilde{P}(Z)\tilde{P}(\chi_{st})$ [2].

The mean value of the scalar dissipation rate can be modelled as:

$$\tilde{\chi} = C_\chi \frac{\tilde{\varepsilon}}{\tilde{k}}\tilde{Z}''^2 \qquad (11)$$

Where $\tilde{k}$ and $\tilde{\varepsilon}$ are the mean turbulent kinetic energy and its dissipation rate, respectively, and C_χ is a constant set equal to 2.0 [2]. The distribution of the scalar dissipation rate, $\tilde{P}(\chi_{st})$, is assumed to be log-normal and the standard deviation for the log-normal distribution of the scalar dissipation rate is set equal to $\sigma_\chi^2 = 2.0$ [2].

NO model

The formation of NO is a slow process, which is kinetically rate limited. Unlike other species, the mean value of NO cannot be obtained from the flamelet library using Eq.10. The concentration of NO is determined by solving its transport equation given by:

$$\frac{\partial}{\partial t}\left(\bar{\rho}\tilde{y}_{NO}\right) + \frac{\partial}{\partial x_k}\left(\bar{\rho}\tilde{u}_k\tilde{y}_{NO}\right) = \frac{\partial}{\partial x_k}\left(\frac{\mu_t}{\sigma_{NO}}\frac{\partial\tilde{y}_{NO}}{\partial x_k}\right) + \bar{\rho}\tilde{\omega}_{NO} \qquad (12)$$

where the turbulent Prandtl number σ_{NO} has been considered to be 0.7. During the flamelet calculation, for a given scalar dissipation rate, the production rate of NO is calculated and tabulated along with other reactive scalars as a function of mixture fraction. The rate of production of NO in the flamelet library is then integrated with presumed PDFs to obtain the mean source term $\tilde{\dot{\omega}}_{NO}$:

$$\tilde{\dot{\omega}}_{NO} = \int\limits_{0}^{\infty}\int\limits_{0}^{1} \dot{\omega}_{NO}\left(Z;\chi_{st}\right)\tilde{P}\left(Z\right)\tilde{P}\left(\chi_{st}\right)dZd\chi_{st} \tag{13}$$

Flamelet library generation

Flamelet library has been generated using FlameMaster code of Pitsch [26]. FlameMaster solves the governing flamelet equations on the mixture fraction space. The effect of differential diffusion of species and radiation heat loss has been neglected and unity Lewis number and equal diffusivity for all the species has been assumed. Reaction mechanisms used for the generation of flamelets are: Peters [27], GRI2.11 [28] and GRI3.0 [29], and San Diego [30]. The Peters mechanism employs reduced chemistry with 53 elementary reactions for the hydro-carbon chemistry in conjunction with the 3 step Zeldovich mechanism of Thermal NO. The GRI 2.11 employs detailed chemistry for both hydro-carbon and nitrogen chemistry and consists of 277 reactions with 49 species. The GRI 3.0 mechanism is a successor to the version 2.11 and comprises of 53 species with 325 elementary chemical reactions (hydro-carbon + nitrogen chemistry). Notable modifications include changes in CH kinetics which are important to the Prompt NO formation. The San Diego mechanism, is relatively new and it has been developed along the similar lines as the GRI 2.11 and GRI 3.0. This mechanism comprises of 52 species with 454 reactions which include detailed nitrogen chemistry.

Burner Geometry

The bluff-body burner used for the simulation was experimentally investigated by Dally et al [31]. The burner has an outer diameter of 50 mm and a concentric jet diameter of 3.6 mm. A wind tunnel with an exit cross-section of 254 mm X 254 mm encloses the burner. Single point Raman/Rayleigh/LIF technique has been used by Dally et al. [31] to measure temperature and the concentration of stable species CO_2, CO, H_2O, H_2, N_2 as well as concentration of OH and CO.

Method of solution

The laminar flamelet model has been applied to simulate a bluff-body stabilised CH_4/H_2 flame, known as HM1 flame, which was experimentally studied by Dally et al [31]. The flame operates at 50% blow-off limit with fuel and co-flow streams at velocities of 118 m/s and 40 m/s respectively, and is devoid of any local extinction phenomenon. Hence, this flame is suitable for the application of laminar flamelet model. CFD simulation has been carried out using an in-house finite-volume code with staggered structured grid arrangement in 2D axisymmetric geometry. Governing equations in cylindrical coordinates have been discretized using hybrid scheme and the discretised algebraic equations have been solved by a line-by-line tri-diagonal matrix algorithm. Pressure-velocity coupling has been achieved by SIMPLE algorithm. Mesh intensity is 162 nodes along axial direction and 111 nodes along radial direction. This mesh size has been chosen after carrying out grid independence study with two finer meshes and one coarser mesh.

Inlet of the domain has been extended by 3 x bluff-body diameters upstream of the burner exit to develop the flow before entry to the reacting zone. At outlet and symmetry, a zero normal gradient condition has been employed, while the bluff-body walls have been subjected to no-slip condition. Near wall turbulence has been specified by using universal log-law of the wall. Further, while employing Reynolds stress model, the near wall Reynolds stresses need to be treated. At the near wall node P,

the normal stresses are derived from near wall turbulent kinetic energy $\tilde{k}_p$ from a closed set of algebraic equations, Eq. 14.The near wall Reynolds shear stress is obtained from the solution of its transport equation.

$$\left(\overline{u''u''}\right)_p^w = 1.098\tilde{k}_p, \quad \left(\overline{v''v''}\right)_p^w = 0.247\tilde{k}_p, \quad \left(\overline{w''w''}\right)_p^w = 0.655\tilde{k}_p \tag{14}$$

Results and Discussions

Mixing and flow field

Figure 1 shows the contour plot of stream function within the bluff-body combustor. Fuel enters the combustor through a central jet, while air enters the combustor through an annular space. As can be seen from Fig. 1, the flow is characterised by two counter rotating vortices at the face of the bluff body. These vortices act to stabilise the flame. The length of the recirculation zone is predicted to be x/D ~ 1.5. Downstream of the recirculation zone is the neck zone. In the neck zone, intense mixing takes place between the fuel jet and the coflow air. Further downstream, the flame expands like a jet flame.

The radial profiles of mean and root mean square (rms) of axial and radial velocity fluctuations for the related HM1e flame are shown in Figs. 2-5. Laminar flamelet model predictions obtained in conjunction with a modified k-ε model [16] have also been plotted in Figs. 2-5. Agreement between the computations and experiment is generally good for the mean axial velocity and there is minor difference between the RST and modified k-ε model. The rms of axial velocity fluctuation is underpredicted by both modified k-ε and RST models, especially near the axis. However, the RST model prediction is much better. Reasonable agreement is achieved for the mean and rms fluctuations of radial velocity.

Thermochemical properties

Figure 6 shows the radial mean mixture fraction profiles at different axial locations. Agreement between the prediction and measurement is good except at x/D=1.8 and x/D=2.4 where, the computed results show minor underprediction in the mean mixture fraction profiles. The prediction of mean mixture fraction at downstream locations (x/D=1.8 and x/D=2.4) has been proved to be challenging. Previous studies using various differential Reynolds stress models (DRSMs) [18], nonlinear k-ε model [19] and even LES [20], failed to predict accurately the mean mixture fraction profile at the farfield. Compared to previous studies of differential Reynolds stress models (DRSMs) [18], the present study provides a much better agreement. The extended upstream flow domain seems to be the main contributor for achieving better prediction. Extended upstream provides realistic development of coflow before it enters the combustor and brings significant improvement of mixing in the outer shear layer. Raman and Pitsch [21] using a recursive filter-refinement procedure (RFRP) for LES, have also shown that LES is capable of predicting downstream mixing field provided the large scale mixing in the outer shear layer is adequately resolved through reliable coflow boundary conditions. Further study is clearly needed to resolve the boundary conditions issue in the coflow to achieve accurate prediction.

The radial profiles of rms of mixture fraction fluctuations are shown in Fig. 7. Agreement between computation and measurement is not as good as for the mean mixture fraction. However, the present study provided a much better agreement compared to various previous studies [18-20].

Radial profiles of mean temperature are shown in Fig. 8. The mean temperature profiles are reasonably well predicted and there is little difference among the reaction mechanisms of San Diego, GRI 2.11 and GRI 3.0. Peters mechanism produces small overprediction at all measuring stations. At x/D=0.26, the measured temperature in the outer vortex remains at ~1650 K, whereas the computational value shows a gradual increase of temperature from the inner to the outer edge of the outer vortex. Dally at al [16] suggested that the experimental lower mean temperature at the edge of the outer shear layer was due the intermittent

local extinction due to higher shear. However, Kuan and Lindstedt [32] suggested that the experimental probe might not adequately resolve the edge of the outer shear layer. Moreover, the uncertainty in the coflow boundary condition has a profound effect on the simulation result at the edge of the outer vortex close to the bluff-body face. These uncertainties discussed above have also resulted in bimodal prediction of CO_2 (Fig. 10) and the overprediction of OH (Fig. 12) at x/D=0.26. Figures 9 and 10 present the radial profiles of mass fraction of H_2O and CO_2 respectively. While the prediction of mass fraction of H_2O is very good, the prediction of CO_2 is not as good especially at the farfield.

Figure 11 shows the mean CO profiles at different axial locations. The GRI 2.11, GRI 3.0 and San Diego mechanisms reproduce the CO profile reasonably well in the nearfield (x/D<0.9) and are close to each other, while Peters mechanism consistently predicts a lower CO level at all locations. This lower estimation of CO by Peters Mechanism is consistent with the overprediction of CO_2 level compared to other reaction mechanisms (Fig. 10). As explained earlier, the uncertainty in the coflow boundary condition has effected the prediction of the farfied flow field and this also resulted in the discrepancy of CO prediction in the farfield.

Mean mass fraction profiles of OH are shown in Fig. 12. Except at x/D=0.26, the OH level is well reproduced in the simulation by all reaction mechanisms. At x/D=0.26, the OH level is severely underpredicted. As explained above, the reaction zone at the outer shear layer may not be adequately resolved in the experiment. This may partially explain the discrepancy between the experimental and numerical results. At x/D=0.6, the simulation predicts a wider reaction zone for OH compared to the measurement. All reaction mechanisms produced very similar prediction for OH. Kim and Huh [14] also reported very similar prediction with GRI 2.11 and GRI 3.0 mechanisms. Compared to flamelet prediction of Kempf et al [20], and CMC prediction of Sreedhara and Huh [15], the present study provided a better prediction, especially at downstream locations. Kempf et al [20] reported a shift of the peak towards the axis of the

combustor, while Sreedhara and Huh [15] reported a shift away from the axis of the combustor.

Figure 13 shows the radial profiles of NO at different axial locations. It is well known that NO is formed through (a) Thermal or Zeldovich (b) N_2O-intermediate and (c) Fenimore or prompt mechanisms. Thermal mechanism is important in the high temperature region for both hydrocarbon and non-hydrocarbon flames. Prompt NO pathway is important for hydrocarbon flames in rich zone, while N_2O pathway is important in lean zone. In the present study, Peters mechanism only includes the thermal mechanism and this leads to the underprediction of NO by approximately 50%. The GRI 2.11 produces very good prediction of NO, especially in the nearfield. In the farfield, the GRI 2.11 mechanism overpredicts the NO level near the centreline. The agreement achieved by the laminar flamelet model with GRI 2.11 is however much better compared to the 1st order CMC model of Kim and Huh [14] and the 2nd order CMC model of Sreedhara and Huh [15]. In the present study, both San Diego and GRI 3.0 mechanisms overpredict the NO level by a large margin. Kim and Huh [14] also reported large overprediction of NO with GRI 3.0 mechanism. They suggested that considerably higher rate coefficient for the principal prompt NO reaction $CH+N_2=N+HCN$ in GRI 3.0 mechanism is the primary reason for overprediction. Timescales for NO reactions are much slower than those of fuel reactions. This slower reaction rates for NO production is accounted in the present simulation through solving a mass transport equation for NO with the source term obtained from the flamelet library. Despite this simple representation of kinetically controlled NO formation, the agreement achieved in the present study is very encouraging. Inclusion of an unsteady flamelet formulation has shown to improve the NO prediction over a steady state flamelet formulation [33]. Another factor that could influence the overprediction of NO is the non-inclusion of radiation heat loss. Ravikanti et al [34] have shown that although the effect of radiation is negligible on temperature and major species, the inclusion of radiation can improve the NO prediction.

Conclusions

This report presents a numerical investigation of the detailed structure of a bluff body stabilised CH_4/H_2 flame. The chemical reaction in the turbulent flame has been modelled using a steady laminar flamelet model, while the turbulence has been represented by a Reynolds stress transport model. Computational domain included an extended upstream, which allowed realistic development of turbulence at the entry to the combustor. Comparison of Peters, GRI 2.11, GRI 3.0 and San Diego reaction mechanisms has been made under the laminar flamelet modelling framework.

Good agreement has been achieved for the flowfield and thermochemical properties. Little difference has been observed among the reaction mechanisms for predicting mean temperature and major species distribution. However, large difference has been observed in predicting mean NO distribution. Peters mechanism in conjunction with thermal NO route has produced large underprediction, while the GRI 3.0 and San Diego mechanism have produced large overprediction. The GRI 2.11 mechanism has yielded the overall best prediction for mean NO. Remaining discrepancy in the mean NO can be overcome by incorporating an unsteady laminar flamelet model and radiation effects.

References

1. **Jones, W. P. and Whitelaw, J. H.,** Calculations method for reacting turbulent flows: a review. *Combust. and Flame,* 1982, **48**, 1-26.
2. **Peters, N.**, Laminar flamelet models in nonpremixed turbulent combustion. *Prog. Energ. Combust. Sci.*, 1984, **10**, 319-339.
3. **Peters, N**., Laminar flamelet concepts in turbulent combustion. *Proc. Combust. Inst.,* 1986, **21**, 1231-1250.

4. **Bray, K. N. C. and Peters, N.**, Laminar flamelets in Turbulent Flames. In P.A. Libby and F. A. Williams (Eds.), *Turbulent Reacting Flows*, Chapter 2. pp. 63-113. London: Academic Press.

5. **Bilger, R. W.,** Conditional moment closure for turbulent reacting flows. *Physics of Fluids A*, 1993, **5(2)**, 436-444.

6. **Pope, S. B.,** PDF methods for turbulent reactive flows. *Prog. Energ. Combust. Sci.*, 1985, **11**, 119-192.

7. **Pope, S. B.**, Computations of turbulent combustion: progress and challenges. *Proc. Combust. Inst.,* 1990, **23**, 591-612.

8. **Muradoglu, M., Liu, K. and Pope, S. B.**, PDF modelling of a bluff-body stabilized turbulent flame. *Combust. and Flame*, 2003, **132**, 115-137.

9. **Barlow, R. S., Smith, N. S. A., Chen, J. Y. and Bilger, R., W.,** Nitric oxide formation in dilute hydrogen jet flames: isolation of the effects of radiation and turbulence-chemistry submodels. *Combust. and Flame*, 1999, **117**, 4-31.

10. **Kronenburg, A., Bilger, R. W. Kent, J. H**., Second-order conditional moment closure for turbulent jet diffusion flames, *Proc. Combust. Inst.,*1998, **27**, 1097-1104.

11. **Roomina, M. A. and Bilger R. W.**, Conditional Moment Closure (CMC) predictions of a turbulent methane-air jet flame. *Combust. and Flame*, 2001, **125**, 1176-1195.

12. **Mahmud, T., Sangha, S., K., Costa, M. and Santos, A.,** Experimental and computational study of a lifted, non-premixed turbulent free jet flame, *Fuel*, 2007, **86**, 793-806.

13. **Hossain, M. and Malalasekera, W.**, Modelling of a bluff body stabilised CH_4/H_2 flame based on a laminar flamelet model with emphasis on NO prediction, *Proc. Inst. Mech. Eng. Part A: J. Pow. and Energ.,* 2005, **217**, 201-210.

14. **Kim, S. H. and Huh, K. Y.**, Use of the conditional moment closure model to predict NO formation in a turbulent CH_4/H_2 flame over a bluff-body, *Combust. and Flame*, 2002, **130**, 94-111.

15. **Sreedhara, S. and Huh, K. Y.,** Modeling of turbulent, two-dimensional nonpremixed CH_4/H_2 flame over a bluffbody using

first- and second-order elliptic conditional moment closures, *Combust. and Flame*, 2005, **142**, 119-134.

16. **Dally, B. B., Fletcher, D. E. and Masri, A. R.**, Flow and mixing fields of turbulent bluff-body jets and flames. *Combust. Theory and Modelling*, 1998, **2**, 193-219.

17. **Merci, B., Dick, E., Vierendeels, J., Roekaerts, D. and Peeters, T. W. J.**, Application of a new cubic turbulence model to piloted and bluff-body diffusion flames. *Combust. Flame*, 2001, **126**, 1533-1556.

18. **Li, G., Naud, B. and Roekaerts, D.**, Numerical investigation of a bluff-body stabilised nonpremixed flame with differential Reynolds-stress models*. Flow Turbul. Combust.*, 2003, **70**, 211-240.

19. **Yan, J., Thiele, F. and Buffat, M.**, A turbulence model sensitivity study for CH_4/H_2 bluff-body stabilized flames. *Flow Turbul. Combust.*, 2004, **73**, 1-24.

20. **Kempf, A., Lindstedt, R. P. and Janicka**, J., Large-eddy simulation of a bluff-body stabilised nonpremixed flame, *Combust. and Flame*, 2006, **144**, 170-189.

21. **Raman, V. and Pitsch, H**., Large-eddy simulation of a bluff-body-stabilised non-premixed flame using a recursive filter-refinement procedure, *Combust. and Flame*, 2005, **142**, 329-347.

22. **Masri, A. R.,** http://www.aeromech.usyd.edu.au/thermofluids/, cited 11th Dec 2007.

23. **Launder, B.E., Reece, G.J., Rodi, W**., Progress in the development of a Reynolds-stress turbulence closure. *J. Fluid Mech.*, 1975, **68**, 537-566.

24. **Lien, F. S. and Leschziner, M. A.,** Assessment of turbulent-transport models including non-linear RNG eddy-viscosity formulation and second-moment closure for flow over a backward-facing step. *Comput. Fluids.*, 1994, **23**, 983-1004.

25. **Naot, D., Shavit, A. and Wolfshtein, M**., Interaction between components of the turbulent velocity correlation tensor. *Israel J. Tech.*, 1970, **8**, 259-269.

26. **Pitsch, H.**, A C++ computer program for 0-D and 1-D laminar flame calculation.

27. **Peters, N.,** Flame calculations with reduced mechanisms-an outline. In N. Peters and B. Rogg (Eds.), *Reduced Kinetic Mechanisms for applications in combustion systems*, 1993, Chapter 1. pp. 3-14. Berlin: Springer-Verlag.

28. http://diesel.me.berkeley.edu/~gri_mech/new21/version21/text 21.html, cited Dec 11th 2007.

29. http://www.me.berkeley.edu/gri-mech/releases.html, cited 11th Dec 2007.

30. http://www-mae.ucsd.edu/~combustion/cermech/, cited 11th Dec 2007.

31. **Dally, B.B., Masri, A.R., Barlow, R.S. and Fiechtner, G.J.,** Instantaneous and mean compositional structure of a bluff-body stabilized nonpremixed flame. *Combust. and Flame*, 1998, **114**, 119-148.

32. **Kuan, T. S. and Lindstedt, R. P.**, Transported probability density function modeling of a bluff-body stabilised turbulent flame. *Proc. Combust. Inst.*, 2005, **30**, 767-774.

33. **Ravikanti, M., Odedra, A., Malalasekera, W.**, Steady/Unsteady flamelet modelling of NO_x in turbulent bluff-body stabilized non-premixed flames. *Work-in-Progress Abstracts of Proc. Combust. Inst.*, 2006, 31, 337.

34. **Ravikanti, M., Malalasekera, W., Hossain, M. and Mahmud, T.**, Flamelet based NO_x-radiation integrated modelling of turbulent non-premixed flame using Reynolds-stress closure, *Accepted for Flow Turbul. and Combust,* 2008.

Appendix

Nomenclature

C_1, C_2 = model constants in pressure strain term

$C_{\varepsilon 1}$, $C_{\varepsilon 2}$ = model constants in dissipation rate equation

D　　　= diameter of the bluff body

D_{ij}　　= diffusivity

k　　　= turbulent kinetic energy

P_{ij}　　= turbulence production by shear

$P(\ )$　　= probability density function

u_i　　= velocity component

x_i　　= coordinate direction

y_{NO}　　= mass fraction of NO

Z　　　= mixture fraction

δ_{ij}　　= Kronecker delta

ε　　　= dissipation rate of turbulent kinetic energy

ϕ　　　= scalar variables

Φ_{ij}　　= pressure strain rate term

μ_t　　= turbulent viscosity

ρ　　　= density

σ　　　= turbulent Prandtl number

χ　　　= scalar dissipation rate

$\dot{\omega}_{NO}$　　= NO production term

Subscript

st　　　　　　　　　stoichiometric

Superscript

$^{-}$　　　conventional ensemble average

$^{\sim}$　　　density-weighted ensemble average

$^{\prime\prime}$　　　density-weighted fluctuation

FIGURES
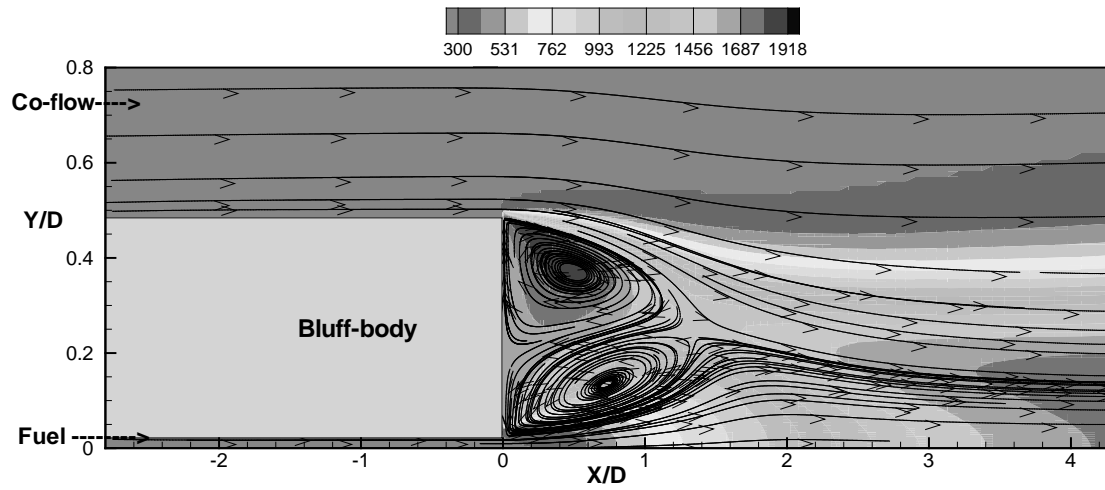
Figure1. Prediction of stream lines superimposed on mean temperature (k) contours in HM1 Flame.
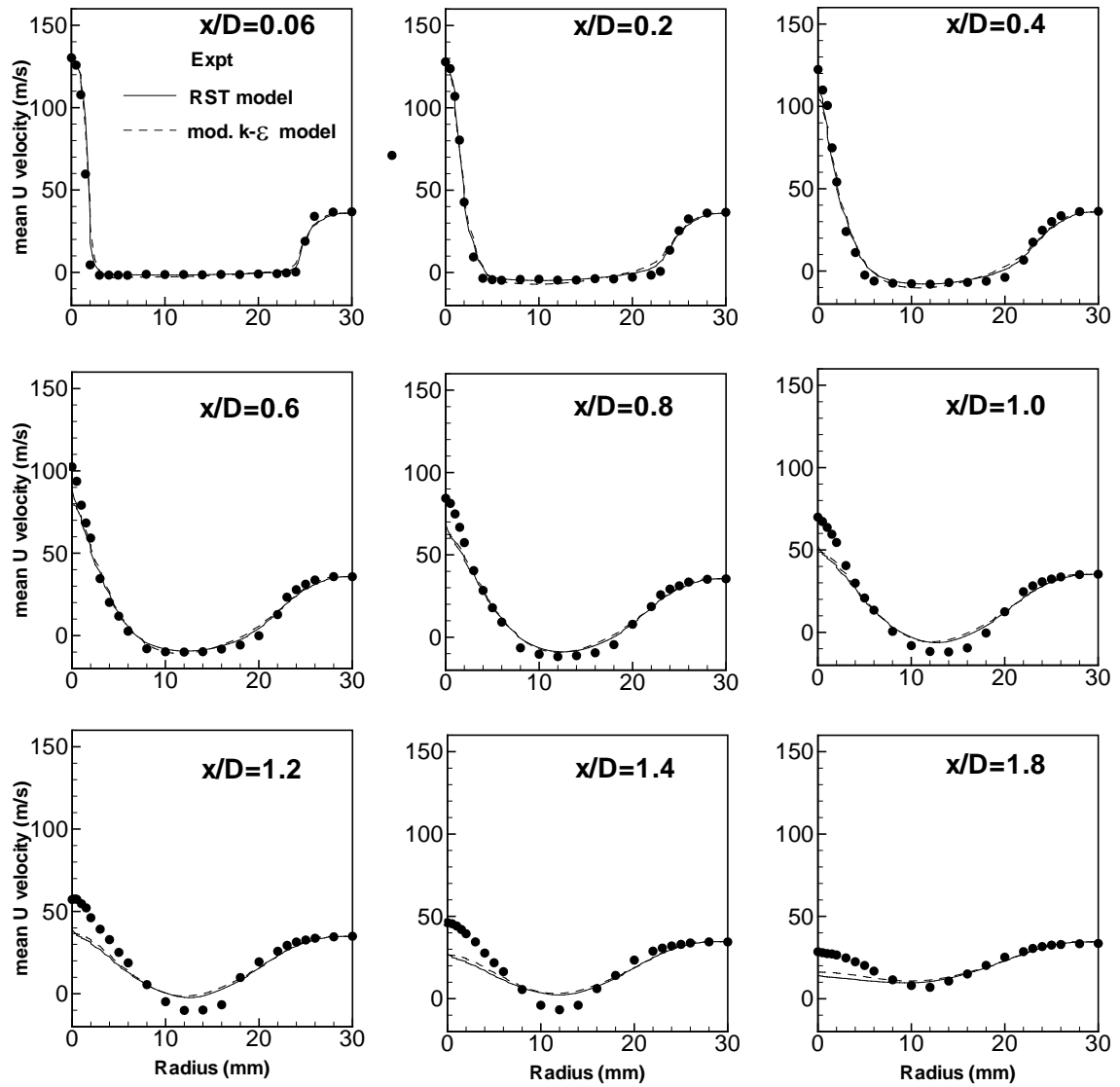
Figure 2: Radial profiles of mean U velocity (m/s)
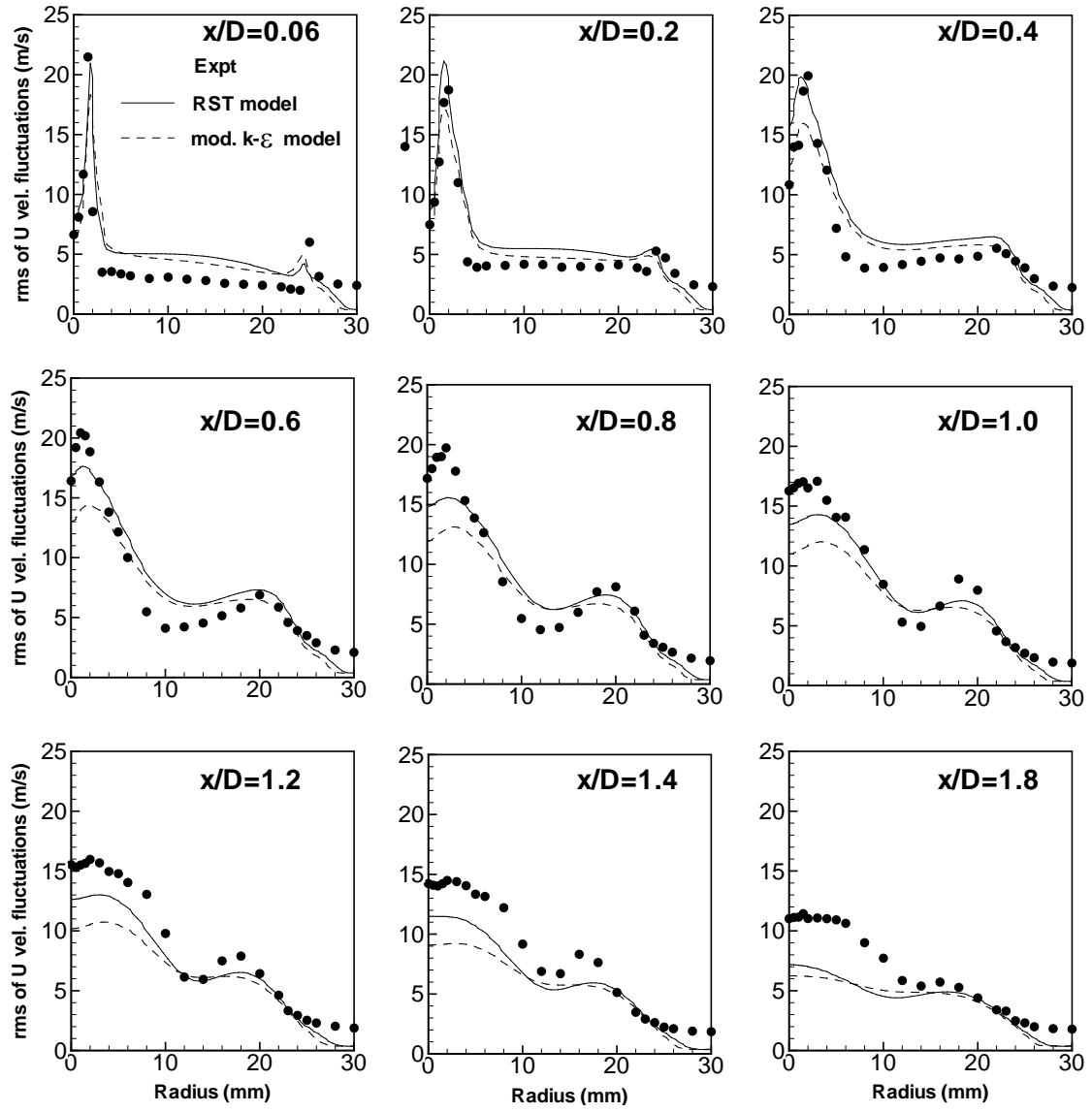
Figure 3: Radial profiles of rms of U velocity fluctuations (m/s)
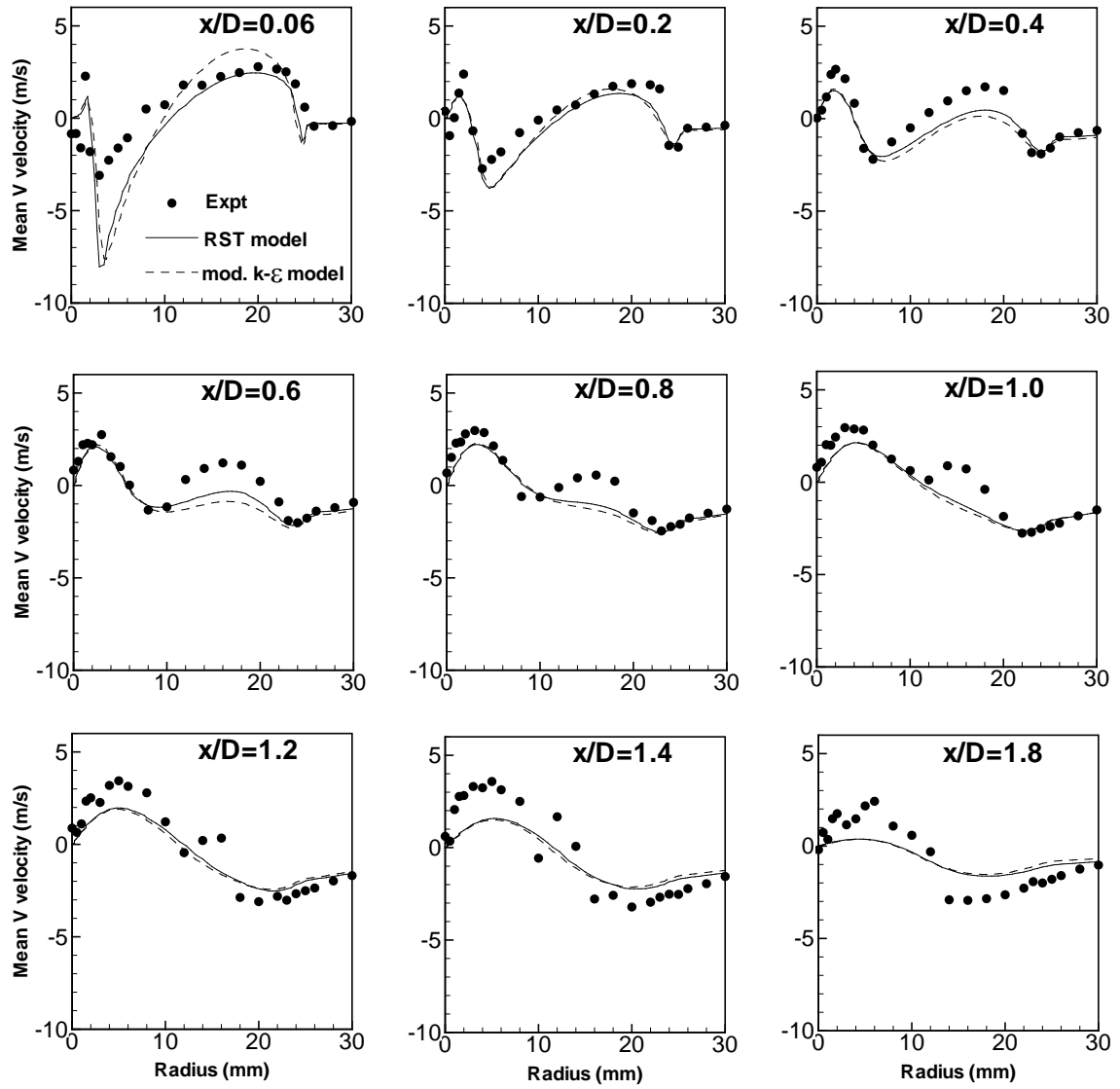
Figure 4: Radial profiles of mean V velocity (m/s)
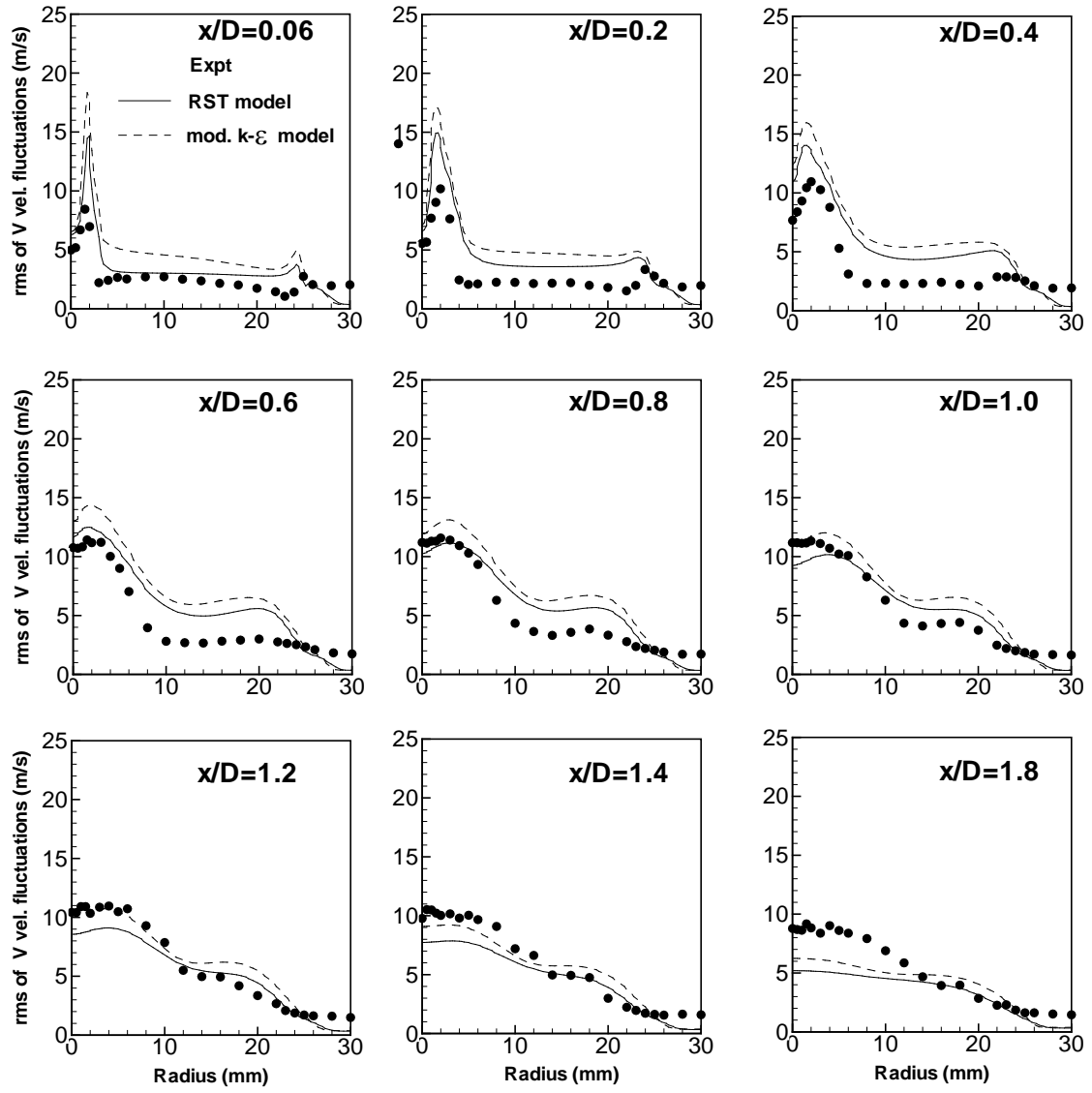
Figure 5: Radial Profiles of rms of V velocity fluctuations (m/s)
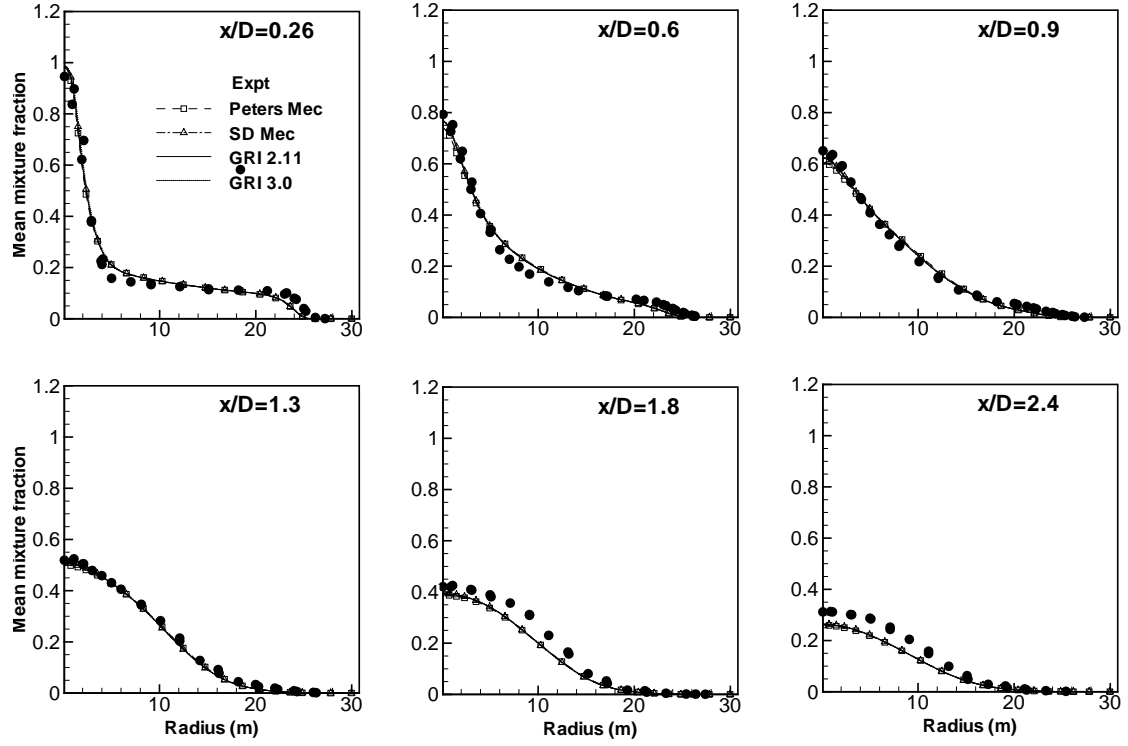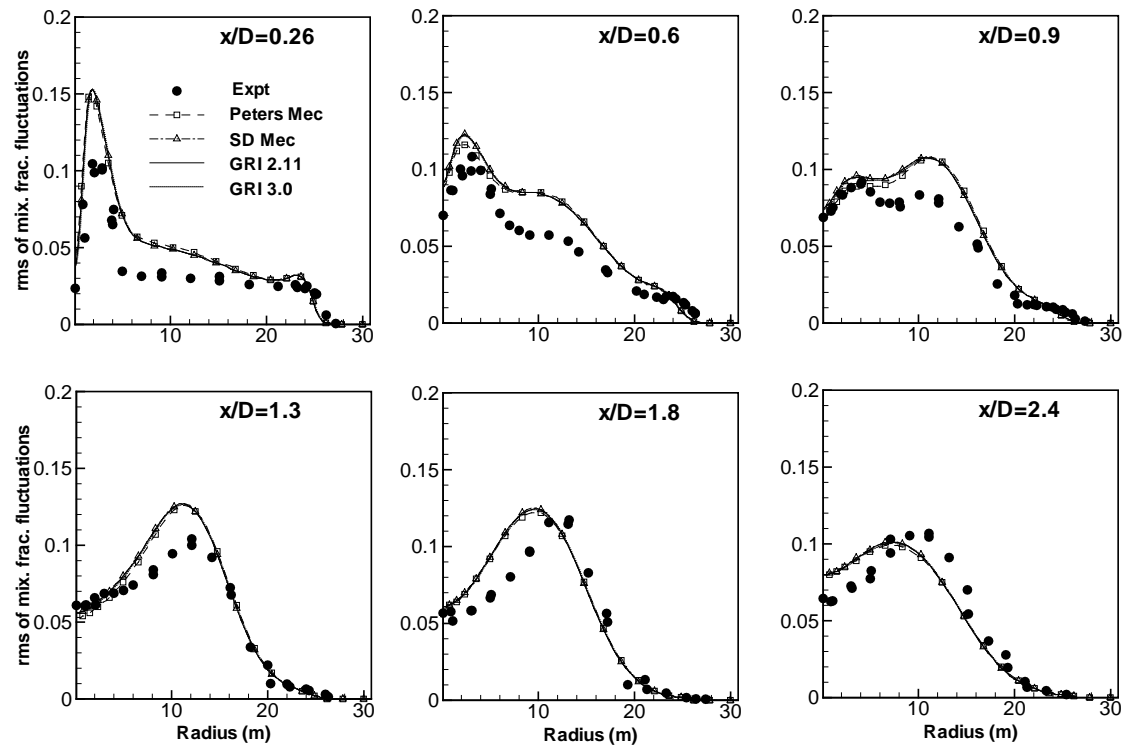
Figure 6: Radial profiles of mean mixture fraction

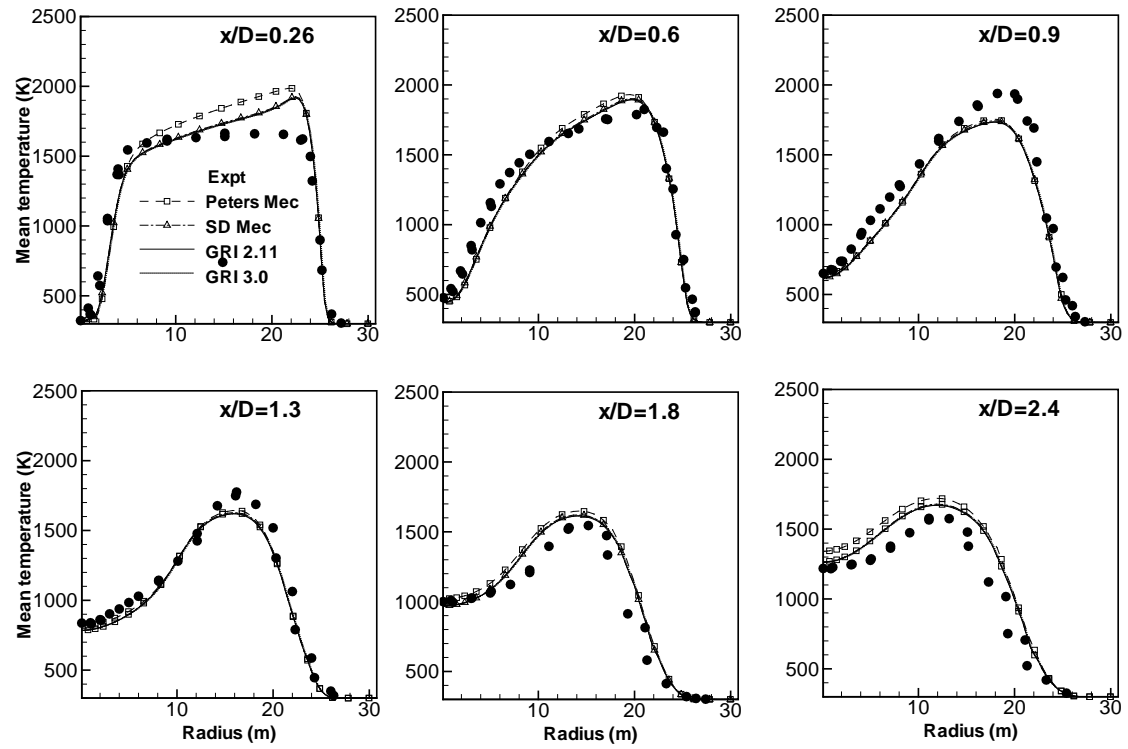

Figure 7: Radial profiles of rms of mixture fraction fluctuations.

Figure 8: Radial profiles of mean temperature (K)
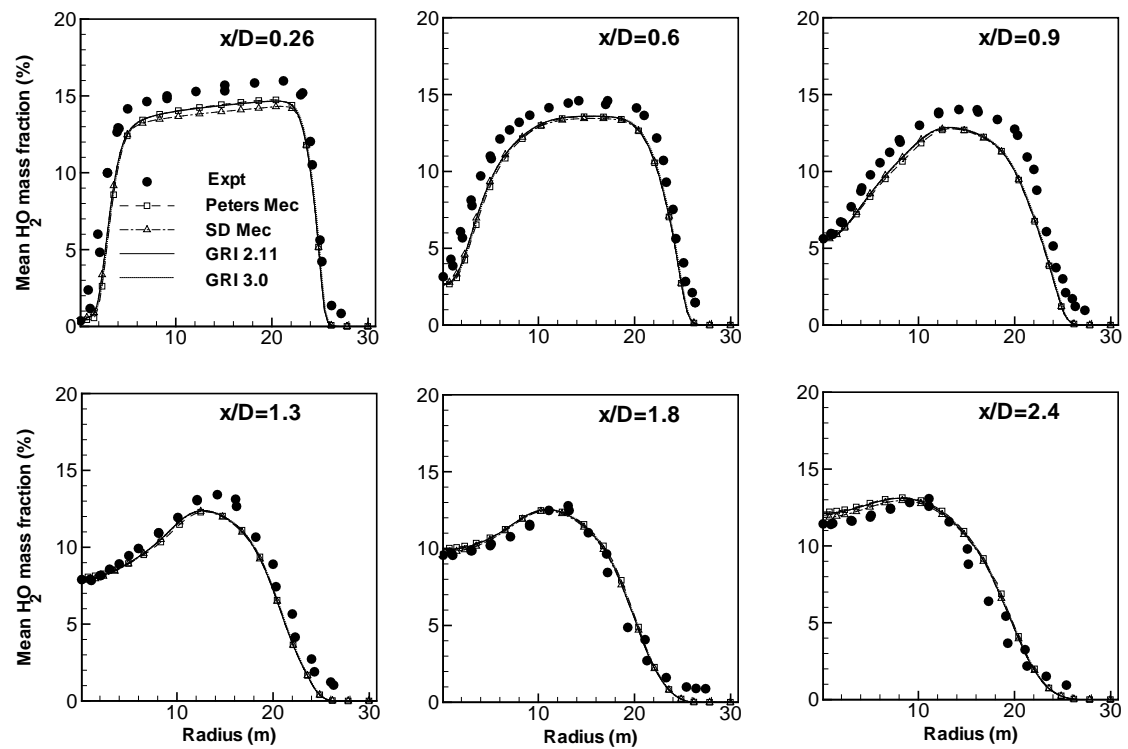
Figure 9: Radial profiles of mean mass fraction of H_2O
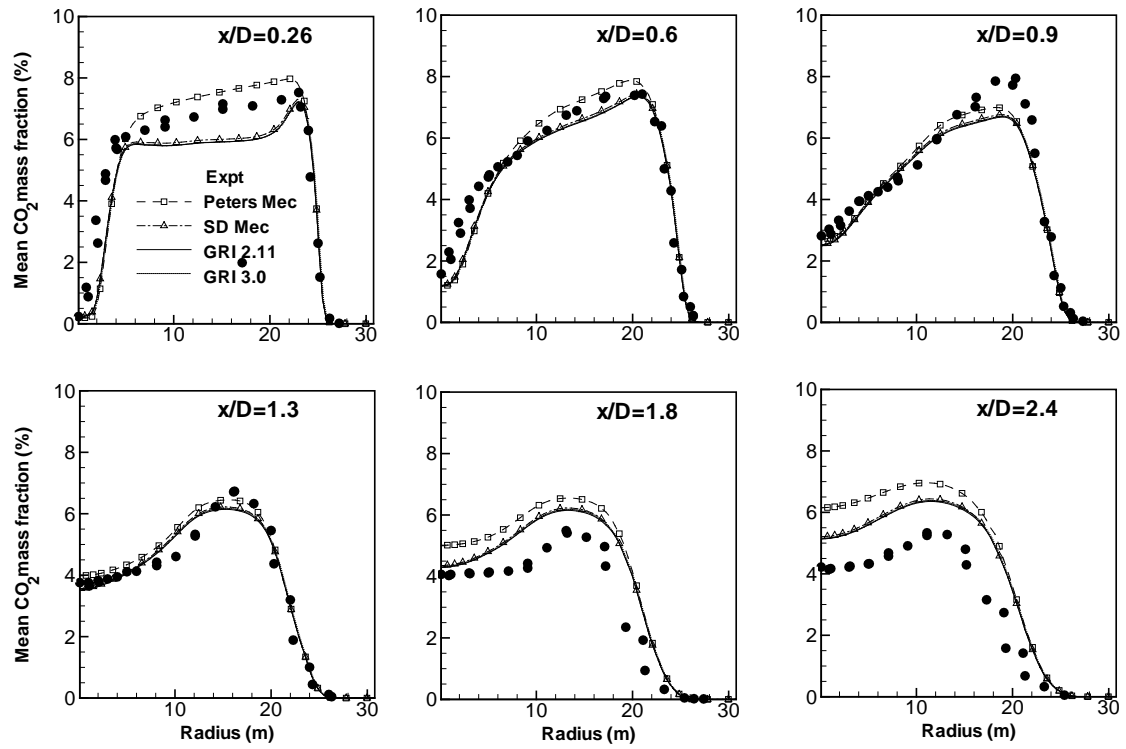
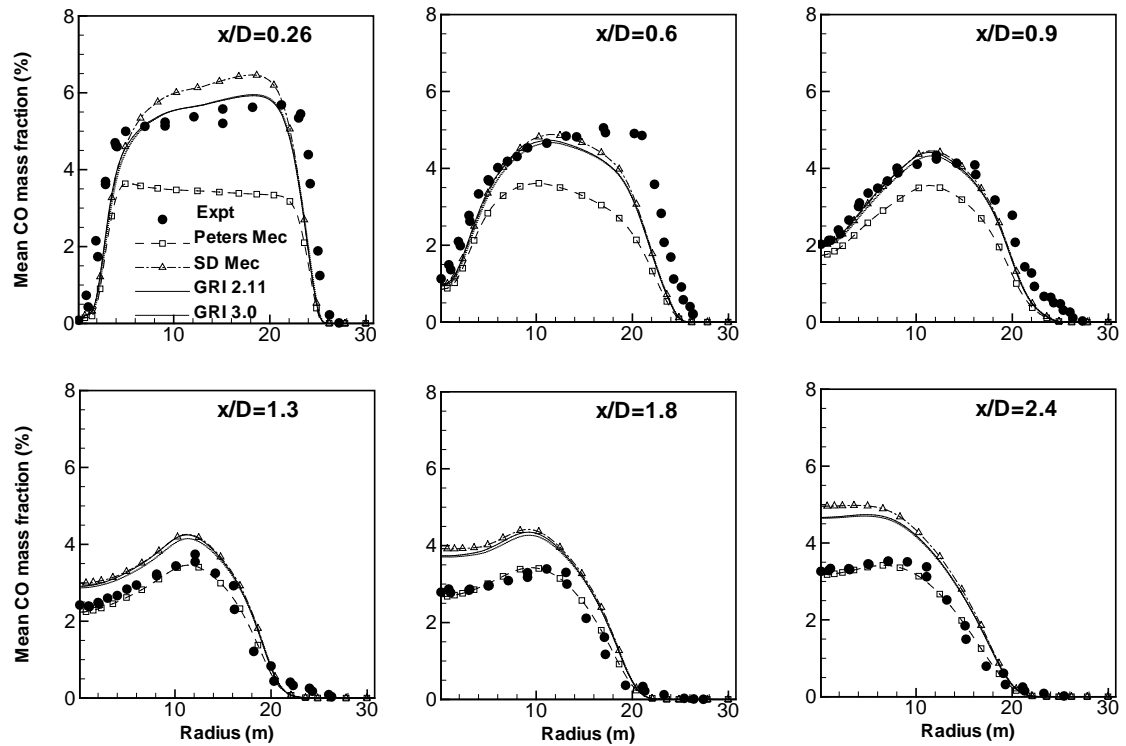**Figure10: Radial profiles of mean mass fraction of CO₂**

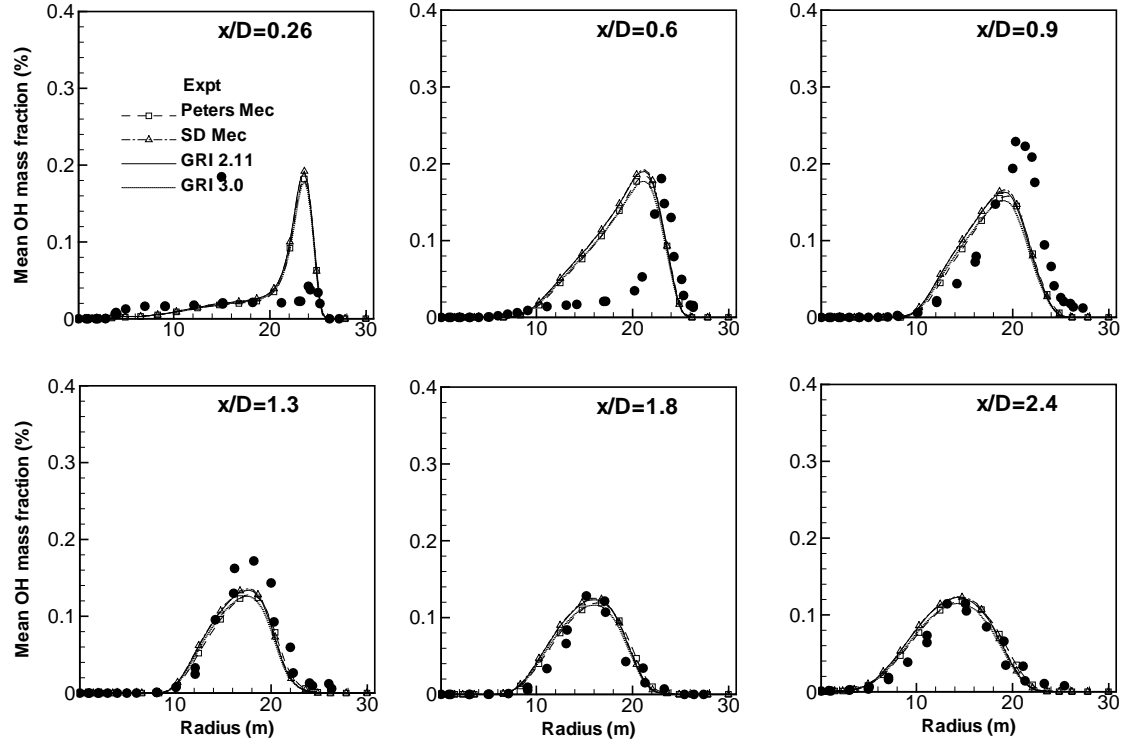**Figure 11: Radial profiles of mean mass fraction of CO**
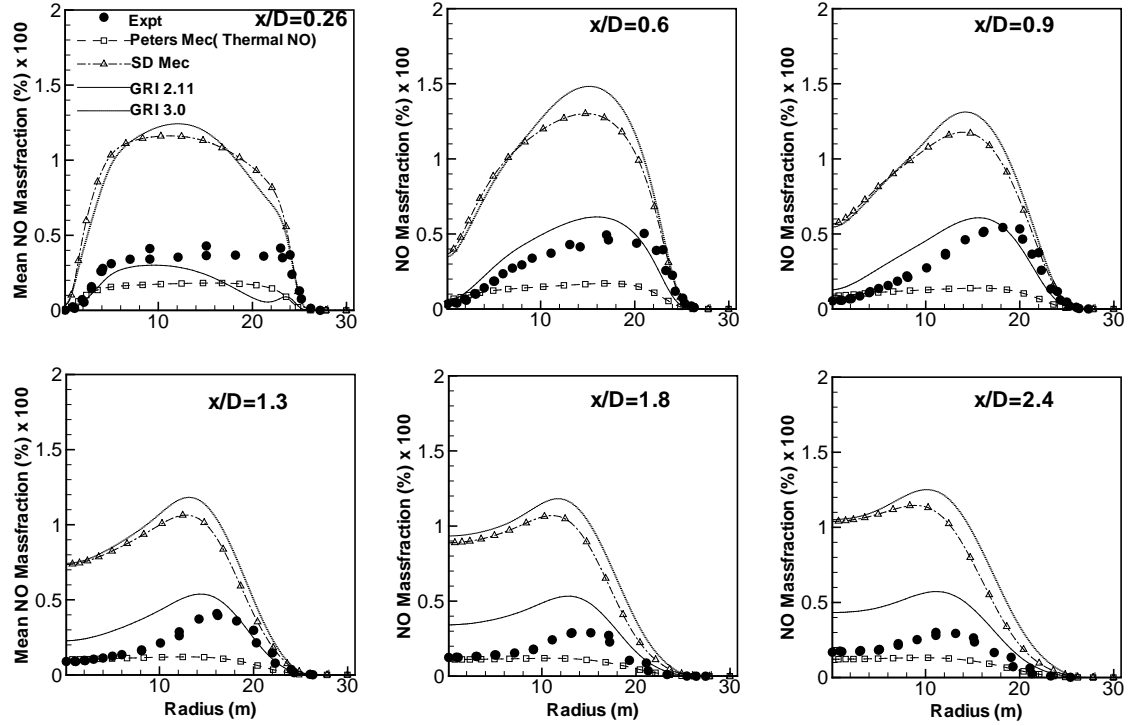
Figure 12: Radial profiles of mean mass fraction of OH

Fig. 13 Radial profiles of mean mass fraction of NO.